Appl Biochem Biotechnol (2010) 162:641–653
DOI 10.1007/s12010-009-8760-3

Kinetic Evaluation of Aminoethylisothiourea on Mushroom Tyrosinase Activity

Shu-Bai Li · Hua-Li Nie · Hai-Tao Zhang · Yong Xue · Li-Min Zhu

Received: 26 June 2009 / Accepted: 17 August 2009 /
Published online: 8 September 2009

Abstract This study demonstrates that aminoethylisothiourea (AET), a potent inhibitor of inducible nitric oxide synthase, is an irreversible competitive inhibitor of mushroom tyrosinase by chelation to the active site of tyrosinase when L-3,4-dihydroxyphenylalanine was assayed spectrophotometrically. The spectrophotometric recordings of the inhibition of tyrosinase by AET were characterized by the presence of a lag period prior to the attainment of an inhibited steady-state rate. The lag period corresponded to the time in which AET was reacting with the enzymatically generated *o*-quinone. Increasing AET concentrations provoked longer lag periods as well as a concomitant decrease in the tyrosinase activity. Both lag period and steady-state rate were dependent on AET, substrate, and tyrosinase concentrations. The inhibition of diphenolase activity of tyrosinase by AET showed positive kinetic cooperativity which arose from the protection of both substrate and *o*-quinone against inhibition by AET. The UV-visible spectrum of a mixture of tyrosinase and AET exhibited a characteristic shoulder peak ascribed to the chelation of AET to the active site of tyrosinase. Moreover, the presence of copper ions only partially prevented but not reverted mushroom tyrosinase inhibition when $CuSO_4$ was added to the assay medium on tyrosinase activity.

Keywords Aminoethylisothiourea · Mushroom tyrosinase · Irreversible inhibition · Cooperativity · Copper chelation

Introduction

Tyrosinase (EC 1.14.18.1) is a multifunctional copper-containing enzyme widely distributed through the phylogenetic scale from lower to higher life forms [1]. Different tyrosinases obtained from various biological sources have similar structural and functional

S.-B. Li · H.-L. Nie · H.-T. Zhang · Y. Xue · L.-M. Zhu (✉)
College of Chemistry, Chemical Engineering and Biotechnology, Donghua University, Shanghai 201620, China
e-mail: lzhu@dhu.edu.cn

characteristics [2]. It is well known that tyrosinase can catalyze two distinct reactions of melanin synthesis, the hydroxylation of monophenol to *o*-diphenol (monophenolase activity) and oxidation of *o*-diphenol to *o*-quinone (diphenolase activity), in both cases by molecular oxygen, and then *o*-quinone also tend to non-enzymatically polymerize melanins [3].

The active site of mushroom tyrosinase contains two copper atoms and exists in three enzymatic forms: mettyrosinase, deoxytyrosinase, and oxytyrosinase [4]. Oxytyrosinase has monophenolase activity, both mettyrosinase and oxytyrosinase have diphenolase activities, deoxytyrosinase can combine with oxygen, and mettyrosinase has no monophenolase activity but has an affinity for substrate; this may explain the occurrence of lag period. Tyrosinase is the critical rate-limiting enzyme in the melanin biosynthesis pathway. Tyrosinase is produced only by melanocytic cells and its synthesis and subsequent processing in endoplasmic reticulum and Golgi, wherein melanin pigment is synthesized and deposited. Excessive or abnormal melanin distribution can cause irregular hyperpigmentation of the skin, such as albinism, melasma, and age spots [5]. Tyrosinase inhibitors, therefore, can be clinically useful for the treatment of some dermatological disorders associated with melanin hyperpigmentation. They also find uses in cosmetics for whitening and depigmentation after sunburn. In addition, tyrosinase is known to be involved in molting, wound healing, skin pigmentation, and sclerotization of insects [6]. Hence, it is possible that inhibition of tyrosinase could lead to abrogation of insect defense mechanisms or abnormal body softening, both of which could be used in pest control.

Aminoethylisothiourea (AET) is a drug widely used in the treatment of failure of brain function through its inhibitory effect on inducible nitric oxide synthase [7]. However, other effects have also been reported for AET to reduce activities of lactate dehydrogenase and liver transaminase but no effects of other enzymes such as xanthine oxidase, catalase, cytochrome P450, or superoxide dismutase [8].

AET in aqueous solution can rearrange to aminothiazoline and 2-mercaptoethylguanidine (MEG). MEG is a thiol compound, and compounds containing thiol groups have long been known to inhibit melanin formation, and they act under certain conditions as depigmenting agents [9, 10]. Moreover, some thiol-containing drugs, such as captopril, penicillamine, and methimazole, have inhibitory effect of tyrosinase [11]. However, the possible effect of AET on tyrosinase activity has not been described so far. The aim of this work is to study, in vitro, the effect of the drug AET on mushroom tyrosinase. This effect includes the inhibition of both monophenolase and diphenolase activities as well as the interaction of AET with the enzymatic catalysis products (*o*-quinones) to form colorless conjugates. These effects have not been reported previously in the literature. This research could provide a possible use for AET as a pharmaceutical additive to avoid hyperpigmentation.

Materials and Methods

Reagents

AET was provided by Yetai Fine Chemical Research Institute (Changzhou, China). L-3,4-dihydroxyphenylalanine (L-DOPA) was purchased from Scholar Bio-Tech Co. (Shanghai, China). Catechol and caffeic acid were supplied by Sinopharm Chemical Reagent Co. (Shanghai, China). All other reagents were of analytical grade.

Re-distillated water was used throughout this research and made traces of free metal ions. Stock solutions of phenolic compounds were prepared freshly everyday in 0.1 M

Na_2HPO_4-NaH_2PO_4 buffer pH 6.8 as solvent to prevent auto-oxidation. Stock solution of AET was prepared in re-distillated water.

Enzymes

"Mushroom tyrosinase" was used in many investigations on inhibition kinetics [12–14]. Full active mushroom tyrosinase is obtained from Sigma (St. Louis, MO, USA). Enzyme solution was prepared in 0.1 M Na_2HPO_4-NaH_2PO_4 buffer pH 6.8 and stored at 4°C.

Kinetic Assays

All the studies in this paper were carried out at least in triplicate.

The mushroom tyrosinase activity on L-DOPA was determined by spectrophotometrically measuring the rate of dopachrome formation at 475 nm with the molar absorption coefficient of 3,700 M^{-1} cm^{-1} by using a UNICO UV-2102PC spectrophotometer (Shanghai, China) [15]. Temperature was controlled at 30°C using a Yiheng MP-5H electric heat constant temperature water box (Shanghai, China) circulating bath with a heater/cooler and was checked using a digital thermometer with a precision of ±0.1°C. This temperature was chosen to increase dopachrome stability. Steady-state rate (V_{ss}) was defined as the slope of the linear zone of dopachrome accumulation curve. One unit of tyrosinase activity was defined and expressed as the amount of enzyme that produced 1 μmol of dopachrome per minute at 30°C. The lag period was determined by extrapolation of the linear portion of the dopachrome accumulation curve to the abscissa axis. All the experiments were performed in 0.1 M Na_2HPO_4-NaH_2PO_4 buffer pH 6.8. The final reaction volume of the assay mixture was 3 ml. All of the assays were carried out under saturating conditions of tyrosinase by molecular oxygen (0.26 mM oxygen in the assay medium) [16].

Inhibition Assays

Inhibition reactions were started by the addition of tyrosinase. This approach was carried out to estimate the continuous effect of AET on the enzyme activity. The assay mixture without AET and enzyme was incubated at 30°C for 10 min.

The inhibition ratio of tyrosinase activity was calculated as follows [17]: $i(\%) = (A - B)/A \times 100$. Here, A and B represent absorbance value for the blank and inhibitor at 475 nm, respectively. The concentration of AET at which 50% of enzyme activity was inhibited (IC_{50}) was obtained.

Non-enzymatic Generation of the Quinone-AET Complex

One hundred micromolar catechol, caffeic acid, or L-DOPA was oxidized by 100 μM sodium-*m*-periodate ($NaIO_4$). The different spectra obtained in the absence and presence of 100 μM AET was recorded in the described spectrophotometer.

Kinetic Data Analysis

To corroborate the direct inhibition of the enzyme by AET, different concentrations of enzyme were added to the pre-incubated mixture as the concentrations of AET increased. The inhibition type was assayed by Lineweaver–Burk plot.

Kinetic cooperativity by nonlinear regression fitting of the experiment data (in the presence of AET) to the Hill equation is as follows:

$$V_{ss} = \frac{V_m [S]_0^h}{K_H^h + [S]_0^h}$$

where h is the Hill coefficient which is a measure of the degree of cooperativity, and K_H is the Hill constant (the microscopic dissociation constant). Nonlinear regression fittings were carried out using Origin software (OriginLab Corporation, USA) for data analysis.

Protein Determination

Protein concentration was determined according to dye-binding method of Bradford [18], using bovine serum albumin (Sigma, St. Louis, MO, USA) as standard.

Results and Discussion

Non-enzymatic Interaction of AET with *o*-Quinones

To elucidate whether the attack of AET to *o*-quinones involved oxidoreduction with regeneration of the corresponding *o*-diphenol or the addition of AET to the *o*-quinone generated a new conjugate, the catechol was oxidized by $NaIO_4$ in the absence and presence of AET. The different spectra were recorded (Fig. 1a). AET alone did not show any characteristic peak (curve a, Fig. 1a). The oxidation of catechol (curve b, Fig. 1a, with λ_{max} at 276 nm) by $NaIO_4$ gave rise to the corresponding *o*-quinone (curve c, Fig. 1a, with λ_{max} at 391 nm). When AET was added to *o*-quinone, a fast disappearance of the maximum of the spectrum at 339 and 391 nm occurred, and no new peak appeared as well as a slight

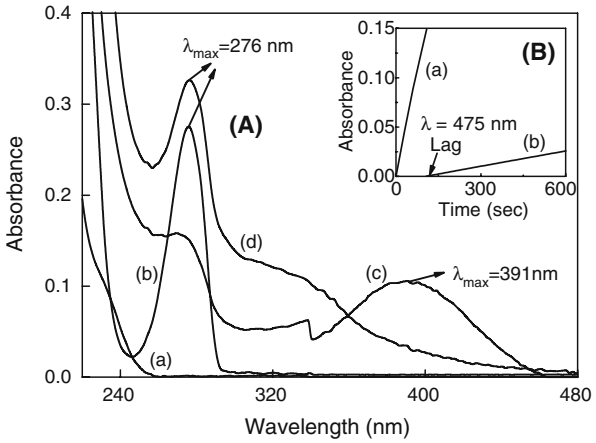

Fig. 1 **a** Scan spectra for aminoethylisothiourea (AET; *a*), catechol (*b*), *o*-quinone (*c*), and the complex *o*-quinone-AET (*d*). Conditions were as follows: 0.1 M Na_2HPO_4-NaH_2PO_4 buffer pH 6.8 and (*a*) 100 μM AET alone, (*b*) 100 μM catechol alone, (*c*) b+ 100 μM $NaIO_4$ = 100 μM *o*-quinone, and (*d*) c+ 100 μM AET = 100 μM *o*-quinone-AET complex. **b** Spectrophotometric recordings for the accumulation of *o*-dopaquinone at 475 nm. Conditions were as follows: 0.1 M Na_2HPO_4-NaH_2PO_4 buffer pH 6.8, 1.0 mM L-DOPA, 60 μM AET, and 2.2 μg/ml tyrosinase

increase at 276 nm (curve d, Fig. 1a). This interaction appears to take place by means of a potent nucleophilic attack of AET through its thiol-containing rearrangement, MEG, to *o*-quinone, as previously described for other thiol compounds [11, 19–22]. It is concluded from this experiment that there was no generation of *o*-quinone after ATE was added in the reaction system, but there was formation of new colorless conjugates. In theory, the attack of MEG could occur the *ortho* or *meta* positions of the ring of *o*-quinone.

The same experiment was carried out with caffeic acid. Caffeic acid alone showed two peaks at 287 and 313 nm. When caffeic acid was oxidized by $NaIO_4$, it showed a new peak at 411 nm to the corresponding *o*-quinone, and at the same time, a fast disappearance of the peak at 287 nm and a slight decrease at 313 nm occurred. When AET was added to *o*-quinone, a fast disappearance of the peak at 411 nm occurred as well as a fast appearance of the peaks at 287 and 313 nm (results not shown). L-DOPA was investigated to interact with AET in this paper. It is known that *o*-dopaquinone undergoes a fast intramolecular cyclization to yield leukodopachrome which was oxidized by another molecule of *o*-dopaquinone to render dopachrome [1, 23]. This aminechrome is relatively stable in the medium, although it may eventually be converted into melanins. AET could compete by means of a nucleophilic attack with internal cyclization preventing dopachrome formation.

The mechanism which describes the effect of AET on both tyrosinase activity and *o*-quinone evolution can be expected in Scheme 1. In Scheme 1, path A described the evolution of *o*-dopaquinone in the addition of AET. The nucleophilic attack of MEG on *o*-quinone, theoretically, can be carried out at three different positions of the *o*-dopaquinone ring; path B described the evolution of *o*-dopaquinone to melanins. Path A is predominant until AET is depleted in the medium, then, pathway B occurs. It was demonstrated with L-DOPA as substrate that the appearance of the lag period in the product accumulation curve (Fig.1b). Kinetic assay was performed at 475 nm. The kinetic courses of the oxidation of L-DOPA in the absence and presence of AET are respectively shown. In the absence of AET (control), the absorbance was immediately recorded at 475 nm by the addition of the enzyme (curve a, Fig. 1b). In the presence of AET, the increase in absorbance was coincident with the characteristic lag period when *o*-dopaquinone accumulation was recorded in the presence of AET (curve b, Fig. 1b). An increase in the absorbance at 475 nm was detected, when AET was depleted in the medium. If AET only inhibited the diphenolase activity of tyrosinase, only the decrease of steady-state rate (V_{ss}, i.e., the slope of absorbance-time curve) was observed, but obviously, lag period in this reaction system was recorded (curve b, Fig. 1b).

Inhibition Effect of AET on Tyrosinase

The assay condition involved the addition of mushroom tyrosinase as the last component of the assay mixture. Absorbance of product accumulation for diphenolase activity of the enzyme on L-DOPA, in the presence of AET, was characterized by the presence of lag period prior to the attainment of a steady state (Fig. 2). AET can inhibit tyrosinase with decreasing of the steady-state rate and lengthening the lag period. There was a marked lag period in Fig. 2. Increasing AET concentrations provoked an increase of the lag period with an increase of inhibition ratio (Fig. 3). The inhibition ratio (curve a, Fig. 3) obviously increased with increasing concentrations of AET. When the concentration of AET reached to 54.0 μM, the inhibition ratio was determined to be 67.0%. Therefore, IC_{50} was estimated to be 45.2 μM. On the other hand, the lag period (curve b, Fig. 3) was extended with increasing concentrations of AET and was estimated to be 68 s in the presence of 54.0 μM. The presence of a lag period in the production accumulation curves was due to the

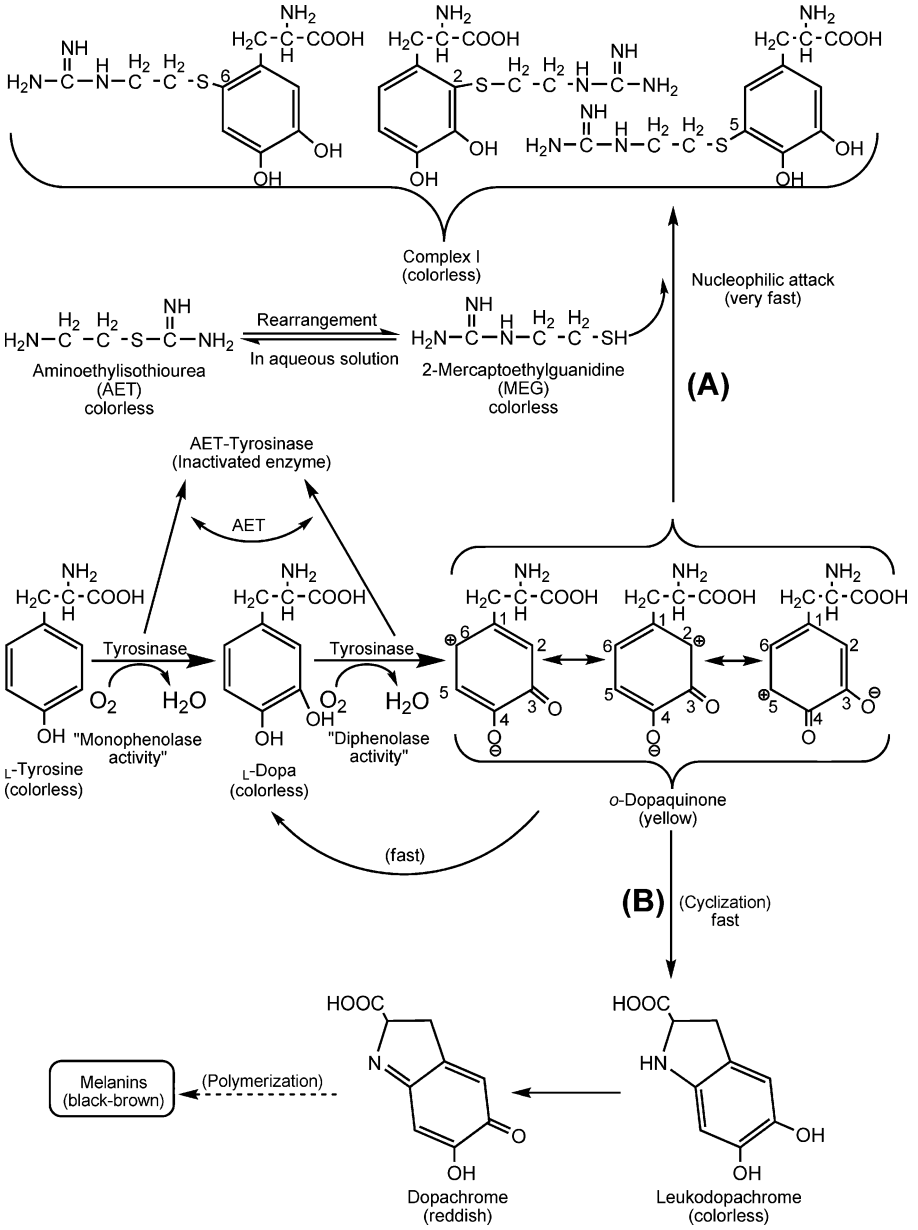

Scheme 1 Mechanism which describes the effect of aminoethylisothiourea (AET) on both tyrosinase activity and *o*-quinone evolution. *A*: evolution of *o*-dopaquinone in the presence of AET. *B*: evolution of *o*-dopaquinone to melanins. Pathway *A* is predominant until AET is depleted in the medium, then path *B* occurs

interaction of MEG with the enzymatically generated *o*-quinones as demonstrated above. When AET was depleted after some time, with the accumulation of the enzymatic products, then the curve rose linearly and gave an invariable slope, the system reached the steady-state rate.

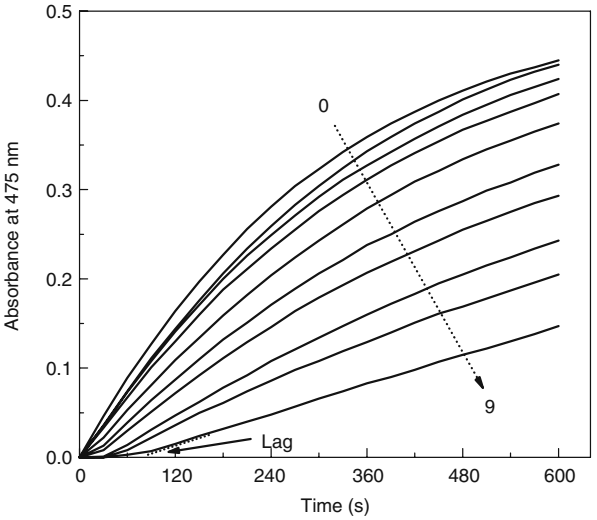

Fig. 2 Progress curves for the inhibition of mushroom tyrosinase by aminoethylisothiourea (AET). The concentrations of AET for curves 0–9 were 0, 6.0, 12.0, 18.0, 24.0, 30.0, 36.0, 42.0, and 48.0 μM, respectively. Assay conditions were 3 ml reaction system containing 1.0 mM L-DOPA and different concentrations of AET in 0.1 M Na_2HPO_4-NaH_2PO_4 pH 6.8 at 30°C. Final concentration of tyrosinase was 2.2 μg/ml

Inhibition Mechanism of AET on Tyrosinase

To corroborate the direct inhibition of the enzyme by AET, V_{ss} were determined by assaying different concentrations in the presence of different AET concentrations (Fig. 4). Tyrosinase activity was linearly dependent on tyrosinase concentration, but the straight lines after linear regression fitting of the experimental V_{ss} values did not pass through the origin when AET concentrations were increased. The plots gave a family of parallel straight lines with same slopes and different abscissa intercepts. This demonstrated the irreversible character of the inhibition of tyrosinase by AET.

Kinetic Data Analysis

Cooperativity is one of the "paradigms" in enzyme kinetics [24] and molecular biology [25], indicated by the sigmoid shape of the plot of product rate against substrate concentration. Its

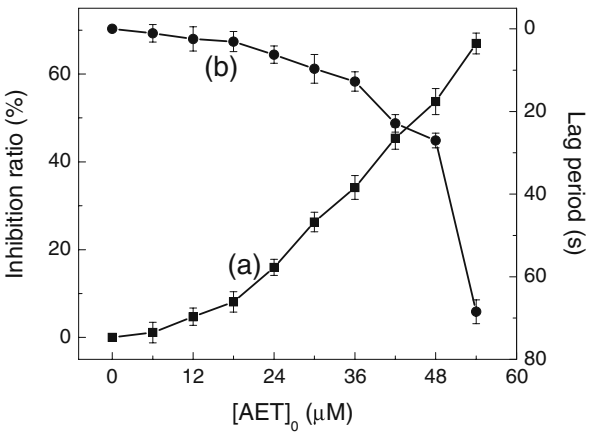

Fig. 3 Effects of aminoethylisothiourea on the inhibition ratio (curve *a*) and the lag period (curve *b*) of mushroom tyrosinase. Conditions were as in Fig. 2

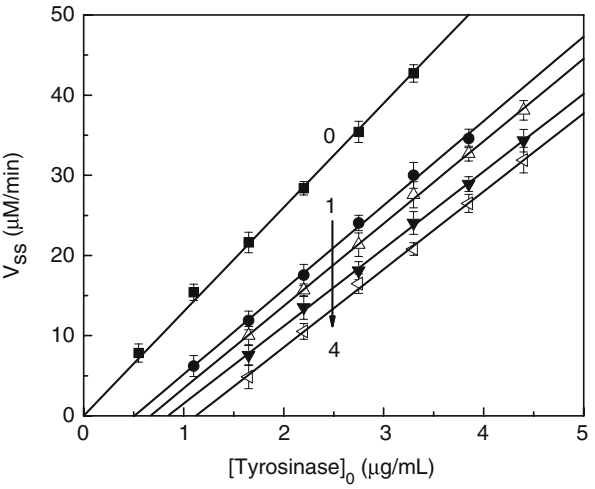

Fig. 4 Dependence of V_{ss} on tyrosinase concentration in the presence of different aminoethylisothiourea (AET) concentrations at 30°C. The concentrations of AET for curves 0–4 were 0 (control), 6.0, 12.0, 18.0, and 24.0 μM, respectively. Conditions were as follows: 0.1 M Na_2HPO_4-NaH_2PO_4 pH 6.8, 1.0 mM L-DOPA, and different concentrations of AET

importance in biochemical processes is derived from its nonlinear behavior and its connection to biological switch with exceptional sensitivity. In this investigation, the dependence of V_{ss} on L-DOPA concentrations in the presence of AET was studied. This effect was analyzed using the Hill equation [26]. When the Hill coefficient (h) is equal to 1, then the Hill constant (K_H) is equal to the Michaelis constant (K_m) which means that there is no cooperativity.

Kinetic cooperativity, arisen from deferent origins, is a feature previously reported in other inhibition systems [11, 27, 28]. In the inhibition of tyrosinase by AET, the kinetic cooperativity arises from the protective effect of L-DOPA and reaction product against the inhibition (L-DOPA confers to the inhibitory action of AET by binding to the enzyme and also by the conversion of L-DOPA into *o*-dopaquinone which reacts with AET).

K_H increased, and V_m remained constant when L-DOPA was used as substrate in the absence (curve a, Fig. 5a) and presence (curve b, Fig. 5a) of AET. The plot (Fig. 5b) was a true curve with the highest linear portion for data points within the −1 to 1 ordinate range. The nonlinear regression fitting of V_{ss} vs substrate to the Hill equation rendered h values higher than 1, which showed positive kinetic cooperativity.

The Lineweaver–Burk plot ($1/V_{ss}$ vs 1/L-DOPA) represented this cooperativity as concave upward curves instead of the normal straight lines (Fig. 6) [11, 29]. Taking into account that V_m values did not change (Fig. 5a) and both h and K_H increased when AET concentrations were increased (Fig. 7), this meant that this irreversible inhibition was competitive when L-DOPA was used as substrate, and Fig. 6 strongly suggested that AET effectively inhibits the tyrosinase activity by binding to the active site.

To elucidate the tyrosinase inhibition mechanism of AET, its chelation behaviors with a copper ion and tyrosinase were examined. A monophenolic substrate initially coordinates to an axial position of one of the coppers of oxytyrosinase. Rearrangement through a trigonal bipyramidal intermediate leads to *o*-hydroxylation of the monophenol by the bound peroxide, loosing H_2O, and formation of the mettyrosinase-diphenol complex [30, 31]. This complex can either render free diphenol as a first step in the diphenolase cycle or undergo oxidation of the diphenolate intermediate bound to the active center, giving a free quinone and a reduced binuclear cuprousenzyme site (deoxytyrosinase).

Mechanism of tyrosinase inhibition by captopril is explained as reported [11]. AET forms the chelation with copper atom in the enzyme and then irreversibly inactivate the

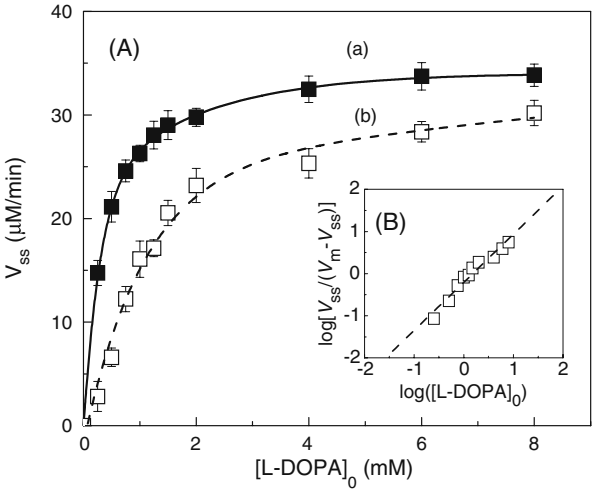

Fig. 5 **a** Dependence of V_{ss} on L-DOPA concentration in the oxidation of L-DOPA catalyzed by tyrosinase in the absence (curve *a*) and presence (curve *b*) of aminoethylisothiourea (AET). Assay conditions were 3 ml reaction system containing different concentrations of L-DOPA and 24 μM AET (curve *b*) in 0.1 M Na_2HPO_4-NaH_2PO_4 pH 6.8 at 30°C. Final concentration of tyrosinase was 2.2 μg/ml. Curves *a* and *b* are nonlinear regression fit of data to Michaelis equation and nonlinear regression fit of data to Hill equation, respectively. **b** Plot of log[V_{ss}/(V_m−V_{ss})] vs log([L-DOPA]); linear regression fit of data from Hill plot with ordinate values within −1 to +1 range

tyrosinase. In the UV-visible spectrum of AET, a characteristic shoulder peak was observed at 250 nm in the presence of copper sulfate ($CuSO_4$), due to chelation for Cu^{2+} (Fig. 8). A similar shoulder peak (230 nm) due to chelation was observed in the mixture of AET and tyrosinase. This indicated that AET could not act as a substrate such as catechin because the behavior was much different from that of catechin and tyrosinase [31–35]. These data strongly suggest the tyrosinase inhibition actions of AET by the chelation to the active site of this enzyme.

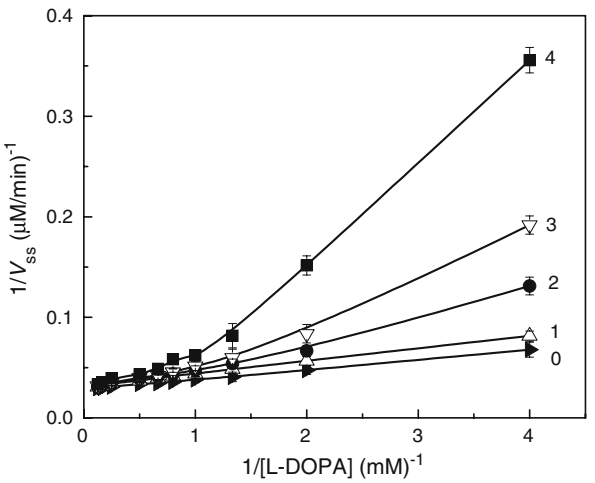

Fig. 6 Lineweaver–Burk plot (1/V_{ss} vs 1/L-DOPA). Conditions were as in Fig. 5 and concentrations of aminoethylisothiourea for curves 0–4 were 0, 6.0, 12.0, 18.0, and 24.0 μM, respectively

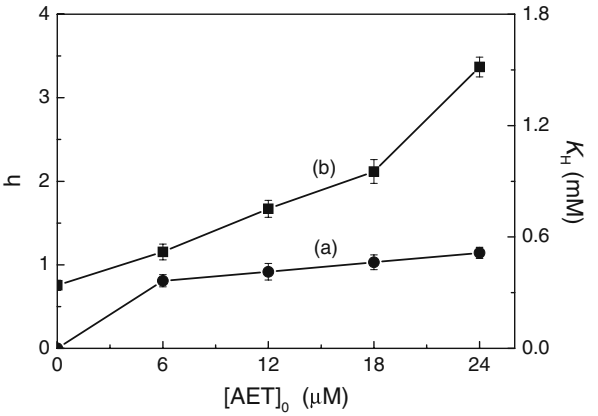

Fig. 7 Dependence of Hill coefficient (*h*; curve *a*) and Hill constant (K_H; curve *b*) for tyrosinase activity in the presence of aminoethylisothiourea. Conditions were as in Fig. 5

To further investigate whether AET exerted its inhibitory effect by chelating the copper atoms at the active site of tyrosinase, $CuSO_4$ was added to the assay medium on tyrosinase activity. When $CuSO_4$ was added to the assay medium before tyrosinase was added, an optimum $CuSO_4$ concentration of 60 μM was able to partially prevent the inhibition of tyrosinase by 24 μM AET (82% of total activity). This was probably due to the formation of a copper-AET complex which did not affect tyrosinase activity (Fig. 9). Lower $CuSO_4$ concentrations were less effective to prevent the inhibition, and higher $CuSO_4$ concentrations provoked a decrease in tyrosinase activity, probably due to a previously reported inhibition of tyrosinase activity due to an excess of copper [11, 36]. Therefore, it is reasonable to think that AET mainly exerts its inhibitory effect by chelating the copper atoms at the active site of tyrosinase. However, as the addition of copper ions was not enough to completely prevent tyrosinase inhibition, it is possible that another mechanism could be involved in the inhibition process. Maybe, the inhibitory process could also involve a disulphide interchange reaction between AET and cysteine rich domains at the active site of the enzyme.

On the other hand, the tyrosinase inhibition by AET is caused by the chelation of AET to tyrosinase, presumably in close proximity to the active site, and accordingly, tyrosinase is inactivated [11, 31, 37]. This is in good agreement with the data of UV-visible spectra; the

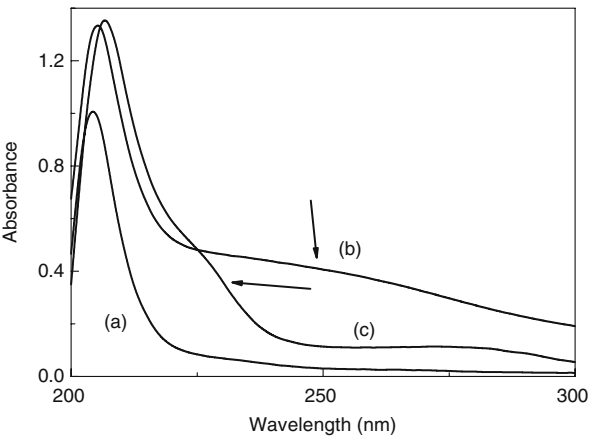

Fig. 8 Scan spectra for aminoethylisothiourea (AET; *a*), AET with $CuSO_4$ (*b*), and AET with tyrosinase (*c*). Conditions were as follows: 0.1 M Na_2HPO_4-NaH_2PO_4 buffer pH 6.8 and (*a*) 100 μM AET alone, (*b*) a+ 100 μM $CuSO_4$, and (*c*) a+ 243 units tyrosinase

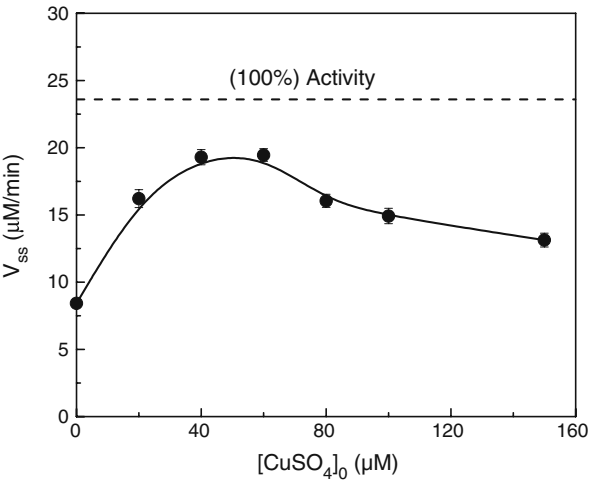

Fig. 9 Dependence of V_{ss} vs $CuSO_4$ concentration before adding tyrosinase to the medium. Conditions were as follows: 0.1 M Na_2HPO_4-NaH_2PO_4 pH 6.8, 1.0 mM L-DOPA, 2.2 μg/ml mushroom tyrosinase, and 24 μM aminoethylisothiourea

chelation of AET to the active site of tyrosinase is clearly demonstrated by the changes of UV-visible spectra induced by the addition of AET.

The chelation of AET to the active site of oxytyrosinase was confirmed to elucidate the monophenolase inhibition mechanism (Fig. 10). When tyrosinase reacted with H_2O_2 in the presence of O_2, mettyrosinase was converted to oxytyrosinase; the characteristic absorption peak of tyrosinase (a mixture of mettyrosinase and oxytyrosinase) centered at 202 nm was shifted to 216 nm, and the absorbance became larger by the addition of an excess of H_2O_2 to tyrosinase (curve b, Fig. 10). In a spectrum of a mixture of AET and oxytyrosinase, the characteristic peaks of AET (204 nm) and oxytyrosinase (216 nm) were shifted to 206 nm by the formation of an AET-oxytyrosinase complex (curve d, Fig. 10). Moreover, like the case of tyrosinase, the characteristic shoulder peak centered at 230 nm was observed. These data suggest that AET truly acts as an inhibitor of oxytyrosinase, not of mettyrosinase.

In summary, safety is a primary consideration for tyrosinase inhibitors, especially those in food and cosmetic products, which may be utilized in unregulated quantities on a regular basis. AET, as a drug, has proven its safety through many years of human use and consumption. Hence, AET described herein may be considered as a potential tyrosinase

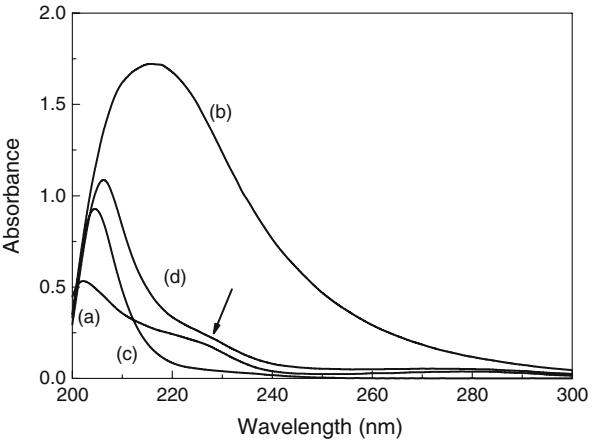

Fig. 10 Scan spectra of tyrosinase (243 units; *a*), oxytyrosinase (243 units; *b*), aminoethylisothiourea (AET; 100 μM; *c*), and AET-oxytyrosinase complex (*d*). Tyrosinase is a mixture of mettyrosinase and oxytyrosinase. Oxytyrosinase is generated by reaction of excess H_2O_2 with tyrosinase in the presence of O_2

inhibitor for food and cosmetic products. The results presented here demonstrate that AET irreversibly inhibits mushroom tyrosinase and also scavenges the generated *o*-quinones, thus preventing melanin formation. This research could shed some light for designing and synthesizing novel potent tyrosinase inhibitors as antibrowning reagents, depigmentation medicine, food preservatives, and cosmetic additives (widely studied such as thiol-containing analogs).

Acknowledgments The present investigation was supported by Natural Science Foundation of China (50773009), Esquel Group, Science and Technology Commission of Shanghai Municipality (08JC1400600), and "111 Project" from Ministry of Education of China (B07024).

References

1. Seo, S.-Y. Sharma, V. K. & Sharma, N. (2003). *Journal of Agricultural and Food Chemistry, 51*, 2837–2853.
2. Rodríguez-López, J. N. Tudela, J. Varón, R. García-Carmona, F. & García-Cánovas, F. (1992). *Journal of Biological Chemistry, 267*, 3801–3810.
3. Sánchez-Ferrer, Á. Rodríguez-López, J. N. García-Cánovas, F. & García-Carmona, F. (1995). *Biochimica et Biophysica Acta. Protein Structure and Molecular Enzymology, 1247*, 1–11.
4. Fenoll, L. G. Peñalver, M. J. Rodríguez-López, J. N. Varón, R. García-Cánovas, F. & Tudela, J. (2004). *International Journal of Biochemistry & Cell Biology, 36*, 235–246.
5. Ando, H. Kondoh, H. Ichihashi, M. & Hearing, V. J. (2007). *Journal of Investigative Dermatology, 127*, 751–761.
6. Wang, S.-D. Luo, W.-C. Xu, S.-J. & Ding, Q. (2005). *Pesticide Biochemistry and Physiology, 82*, 52–58.
7. Szabó, C. Ferrer-Sueta, G. Zingarelli, B. Southan, G. J. Salzman, A. L. & Radi, R. (1997). *Journal of Biological Chemistry, 272*, 9030–9036.
8. Martínez, M. C. Randriamboavonjy, V. Stoclet, J.-C. & Andriantsitohaina, R. (2001). *Biochemical Pharmacology, 61*, 109–118.
9. Vauzour, D. Vafeiadou, K. & Spencer, J. P. E. (2007). *Biochemical and Biophysical Research Communications, 362*, 340–346.
10. da Cruz-Vieira, I. & Fatibello-Filho, O. (1999). *Analytica Chimica Acta, 399*, 287–293.
11. Espín, J. C. & Wichers, H. J. (2001). *Biochimica et Biophysica Acta, 1544*, 289–300.
12. Criton, M. & Mellay-Hamon, V. Le. (2008). *Bioorganic & Medicinal Chemistry Letters, 18*, 3607–3610.
13. Li, B. Huang, Y. & Paskewitz, S. M. (2006). *FEBS Letters, 580*, 1877–1882.
14. Kubo, I. Nihei, K. & Shimizu, K. (2004). *Bioorganic & Medicinal Chemistry, 12*, 5343–5347.
15. Chen, Q.-X. Song, K.-K. Qiu, L. Liu, X.-D. Huang, H. & Guo, H.-Y. (2005). *Food Chemistry, 91*, 269–274.
16. Muñoz, J. L. García-Molina, F. Varón, R. Rodríguez-López, J. N. García-Cánovas, F. & Tudela, J. (2006). *Analytical Biochemistry, 351*, 128–138.
17. Casañola-Martín, G. M. Marrero-Ponce, Y. Khan, M. T. H. Ather, A. Sultan, S. Torrens, F. et al. (2007). *Bioorganic & Medicinal Chemistry, 15*, 1483–1503.
18. Bradford, M. M. (1976). *Analytical Biochemistry, 72*, 248–254.
19. Khym, J. X. Doherty, D. G. & Shapira, R. (1958). *Journal of the American Chemical Society, 80*, 3342–3349.
20. Agrup, G. Hansson, C. Rorsman, H. & Rosengren, E. (1982). *Archives of Dermatological Research, 272*, 103–115.
21. Saito, S. & Kawabata, J. (2004). *Journal of Agricultural and Food Chemistry, 52*, 8163–8168.
22. Awad, H. M. Boersma, M. G. Boeren, S. Van Bladeren, P. J. Vervoort, J. & Rietjens, I. M. C. M. (2003). *Chemical Research in Toxicology, 16*, 822–831.
23. García-Molina, F. Peñalver, M. J. Fenoll, L. G. Rodríguez-López, J. N. Varón, R. García-Cánovas, F. et al. (2005). *Journal of Molecular Catalysis. B, Enzymatic, 32*, 185–192.
24. Cornish-Bowden, A. (2004). *Fundamentals of enzyme kinetics* (3rd ed.). London: Portland.
25. Koshland, D. E. & Hamadani, K. (2002). *Journal of Biological Chemistry, 277*, 46841–46844.
26. Hofmeyr, J.-H. S. & Cornish-Bowden, A. (1997). *Computer Applications in the Biosciences, 13*, 377–385.

27. Espín, J. C. & Tudela, J. (1994). *Biochemical Journal, 299*, 29–35.
28. Duggleby, R. G. (1994). *Biochimica et Biophysica Acta, 1209*, 238–240.
29. Segel, I. H. (1976). *Enzyme kinetics*. New York: Wiley.
30. Lerch, K. (1981). In H. Sigel (Ed.), *Metal ions in biological systems*. New York: Marcel Dekker.
31. Kim, Y.-J. Chung, J. E. Kurisawa, M. Uyama, H. & Kobayashi, S. (2004). *Biomacromolecules, 5*, 474–479.
32. Kermasha, S. Bao, H. & Bisakowski, B. (2001). *Journal of Molecular Catalysis. B, Enzymatic, 11*, 929–938.
33. Moridani, M. Y. Scobie, H. Salehi, P. & O'Brien, P. J. (2001). *Chemical Research in Toxicology, 14*, 841–848.
34. Kubo, I. & Kinst-Hori, I. (1999). *Journal of Agricultural and Food Chemistry, 47*, 4121–4125.
35. Kubo, I. Kinsy-Hori, I. Chaudhuri, S. K. Kubo, Y. Sánchez, Y. & Ogura, T. (2000). *Bioorganic & Medicinal Chemistry, 8*, 1749–1755.
36. Kahn, V. & Andrawis, A. (1984). *Phytochemistry, 24*, 905–908.
37. Bertoldi, M. Gonsalvi, M. & Voltattorni, C. B. (2001). *Biochemical and Biophysical Research Communications, 284*, 90–93.